Organic Process Research & Development **2009**, *13*, 1100–1110

Synthesis of the NK1 Receptor Antagonist GW597599. Part 3: Development of a Scalable Route to a Key Chirally Pure Arylpiperazine Urea, A Happy End

Giuseppe Guercio,*[,†] Sergio Bacchi,*[,†] Alcide Perboni,[†] Corinne Leroi,[§] Francesco Tinazzi,[†] Ilaria Bientinesi,[†] Marie Hourdin,[⊥] Michael Goodyear,[†] Stefano Curti,[†] Stefano Provera,[‡] and Zadeo Cimarosti[†]

Chemical Development and Analytical Chemistry, GlaxoSmithKline Medicines Research Centre, Via Fleming 4, 37135 Verona, Italy, Sanofi-Aventis R&D Centre, 195 route d'Espagne BP 13669, 31036 Toulouse Cedex 1, France, and Pharmasynthese, Process Industrialization - 57 rue Gravetel, 76320 Saint Pierre lès Elbeuf, France

Abstract:

GW597599 1 is a novel NK-1 antagonist currently under investigation for the treatment of central nervous system disorders and emesis. The initial chemical development synthetic route, derived from the one used by medicinal chemistry, involved several hazardous reagents, gave low yields and produced high levels of waste. Through a targeted process of research and development, application of novel techniques and extensive route scouting, a new synthetic route for GW597599 was developed. This paper reports the optimisation work of the third and last stage in the chemical synthesis of GW597599 and the development of a pilot-plant-suitable process for the manufacturing of optically pure arylpiperazine derivative 1. In particular, the process eliminated the use of triphosgene in the synthesis of an intermediate carbamoyl chloride, substantially enhancing safety, overall yield, and throughput.

1. Introduction

Substance P (SP) is a member of the neurokinin family that exerts its pleiotropic role by preferentially binding to the neurokinin receptor classified as NK1.[1] Substance P and the NK1-receptors that mediate its activity are present in the brain stem centres that elicit the emetic reflex. Nausea and vomiting have been reported as the most distressing side effects of chemotherapy, and the disruptive effects of these symptoms on patients' daily lives have been well documented. In light of the need for continued routine use of emetogenic chemotherapy, effective prevention of chemotherapy-induced nausea and vomiting (CINV) is a central goal for physicians administering cancer chemotherapy. GW597599 **1** is a novel NK-1 antagonist currently being developed to relieve these symptoms. This and other NK-1 antagonists have also been investigated for the treatment of CNS disorders such as depression. In this paper we describe the successful efforts to define a synthetic route for large-scale manufacturing.

2. Initial Synthetic Route

The synthetic route used for the synthesis of the first few grams of GW597599 is shown in Scheme 1.

2.1. Experimental Details. The key stage to access the final compound was the coupling between the racemic ketopiperazine **7** and the racemic benzylamine **12** to give the hindered quaternary urea **8** via the synthesis of the carbamoyl chloride intermediate **13**.

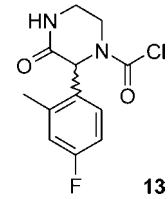

13

To prepare this reactive acyl chloride, the ketopiperazine was treated with the highly toxic triphosgene,[2] in a mixture of dichloromethane and triethylamine followed by addition of benzylamine **12** plus an auxiliary base.

The addition of the benzylamine was followed by a solvent swap between dichloromethane and acetonitrile, allowing shortening of the reaction time by performing the coupling at the acetonitrile refluxing temperature. The base was needed to capture the hydrochloric acid evolved in the step. However, to avoid the risk of losing the triethylamine during the solvent exchange, the higher-boiling *N*,*N*-diisopropylethylamine was also added. The amide group in the piperazine ring was then reduced by treatment with a solution of borane in THF at reflux. The resulting crude product was purified by chromatography to isolate a single diastereoisomer of **1** which underwent a further classical resolution procedure to obtain the optically pure GW597599. The final compound was then crystallized as its pharmaceutically active acetate salt.

2.2. Initial Evaluation of a Possible Enantiospecific Approach. It was evident that the possibility to access the enantiopure ketopiperazine **7**[3] and benzylamine **12** would have produced a single diastereoisomer **14**. However, the attempt to reduce the amide group in the piperazine ring by treatment with a solution of borane in THF at reflux led to the partial epimerization at the chiral centre of this ring (Scheme 2). The proton α to the ureidic moiety, being benzylic in nature, is in fact very acidic.

* Authors to whom correspondence may be sent. E-mail: giuseppe.2.guercio@gsk.com; sergio.k.bacchi@gsk.com.

† Chemical Development, GlaxoSmithKline Medicines Research Centre.

‡ Analytical Chemistry, GlaxoSmithKline Medicines Research Centre.

§ Sanofi-Aventis R&D Centre.

⊥ Pharmasynthese.

(1) Di Fabio, R.; Griffante, C.; Alvaro, G.; Pentassuglia, G.; Pizzi, D. A.; Donati, D.; Rossi, T.; Guercio, G.; Mattioli, M.; Cimarosti, Z.; Marchioro, C.; Provera, S.; Zonzini, L.; Montanari, D.; Melotto, S.; Gerrard, P. A.; Trist, D. G.; Ratti, E.; Corsi, M. *J. Med. Chem.* **2009**, *52*, 3238–3247.

(2) Rosiak, A.; Hoenke, C.; Christoffers, J. *Eur. J. Org. Chem.* **2007**, *26*, 4376–4382.

(3) Guercio, G.; Bacchi, S.; Goodyear, M.; Carangio, A.; Tinazzi, F.; Curti, S. *Org. Process Res. Dev.* **2008**, *12*, 1188–1194.

10.1021/op9002032 CCC: $40.75
Published on Web 10/02/2009

Scheme 1. **Initial synthetic route**

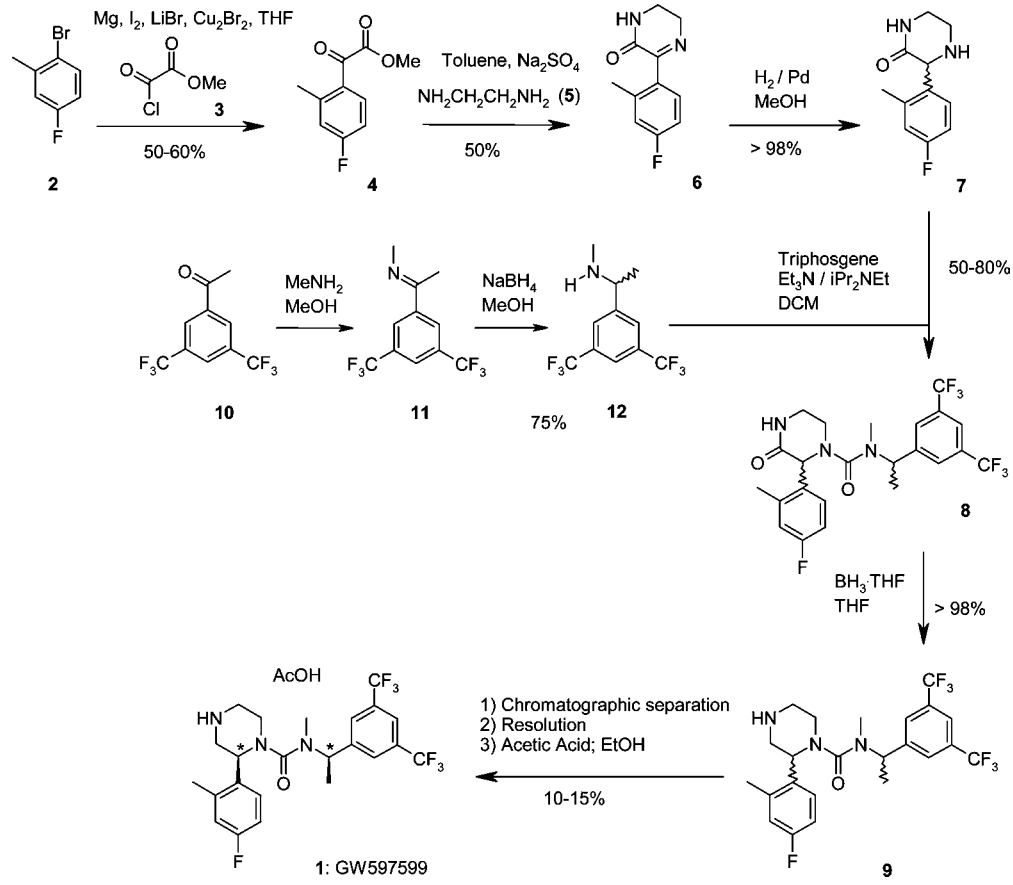

Scheme 2. **Enantiospecific version of the initial synthetic route**

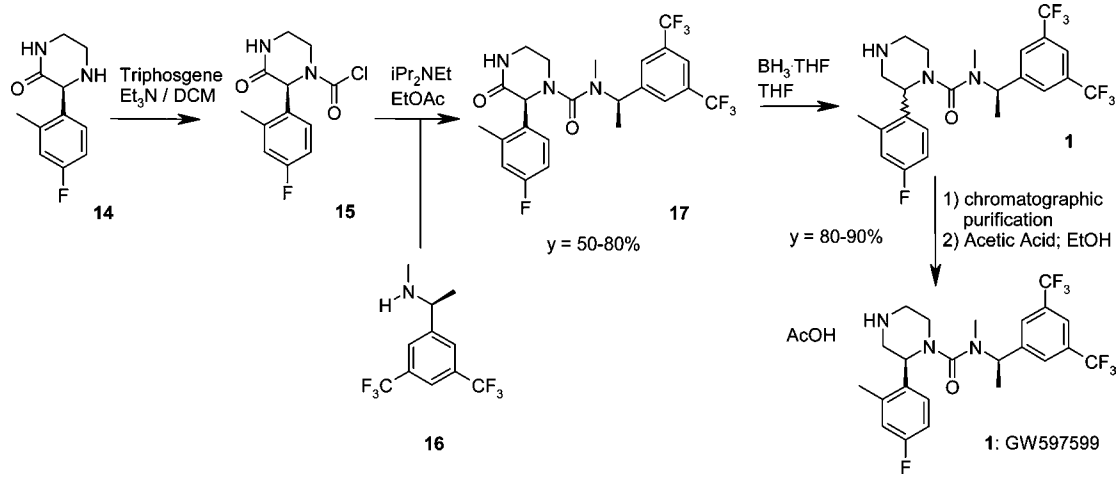

3. Development of a Convergent Process

3.1. Synthetic Strategy. An alternative process to avoid this partial epimerization was envisaged. The disconnection of **1** into the two chiral fragments **16** and **18**,[4] shown in Scheme 3, provided the basis of a more efficient route. This encompassed the need for the last-stage resolution and addressed the issue of the partial racemisation in the final chemical step caused by borane.

Scheme 3. **New potential route**

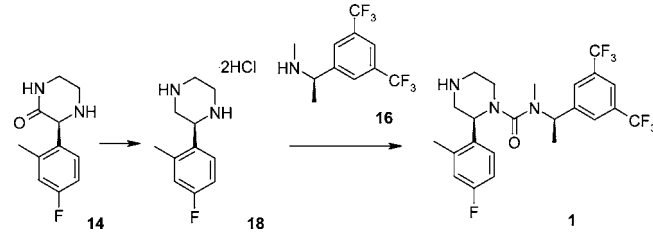

3.2. Development of a Selective Arylpiperazine Nitrogen Monoprotection. The synthesis of the carbamoyl chloride of the piperazine dihydrochloride **18** instead of the keto-derivative **14** required the use of a protecting group to discriminate between the two nitrogen atoms (Scheme 4). Three different protecting groups were tried: 4-nitrobenzylchloroformate (4-

(4) Guercio, G.; Manzo, A. M.; Goodyear, M.; Bacchi, S.; Curti, S.; Provera, S. *Org. Process Res. Dev.* **2009**, 489–493.

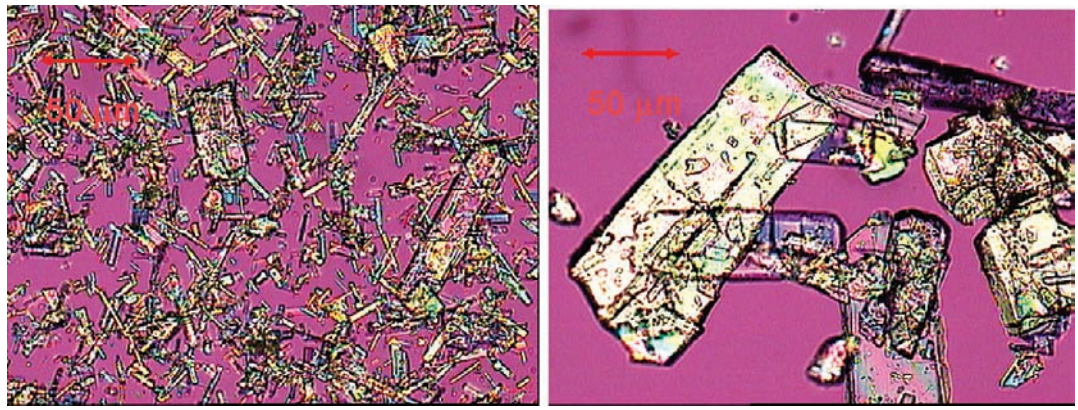

Figure 1. **Optical microscopy (polarized light 125×) of the two different batches of piperazine dihydrochloride 18.**

Scheme 4. **Selective nitrogen monoprotection**

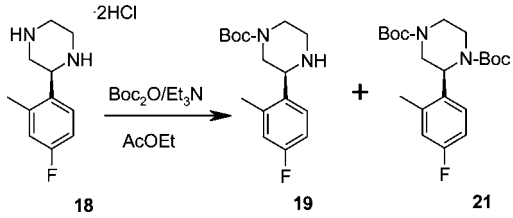

Table 1. **Comparison between different nitrogen protecting groups**

protecting group[a]	area % monoprotected	area % diprotected	area % starting **18**	cost for 1 mmol of protecting agent[b]
4-NBCF	93.0	3.2	3.8	1.15
CbzCl	77.4	8.6	14.0	0.06
Boc_2O	94.0	5.0	1.0	0.39

[a] Note: the protecting agents were used equimolar to the starting material in the same dilution conditions. [b] In euros. Raw material prices were referred to Aldrich catalogue 2009−2010.

NBCF),[5] benzylchloroformate chloride (CbzCl)[6] and di-*tert*-butyl-dicarbonate (Boc_2O).[7] Results for each of those are shown in Table 1.

The balance between selectivity, cost, and ease of removal pointed us toward the Boc_2O.

Surprisingly, when the optimised conditions were applied to two different batches of piperazine **18**, in one case we observed the expected ratio of 94:6 of **19**:**21**, while in the other one a 75:25 ratio was found, with no evident explanation for the decrease in selectivity. Cooling the reaction mixture led to an even worse ratio of about 50:50, with a large amount of unreacted starting piperazine **18** recovered after aqueous workup. A microscopy study highlighted a difference between the two batches that was considered of use in the rationalisation process. The batch that reacted as expected had a smaller particle size distribution with respect to the batch that had a higher amount of diprotected derivative **21**, which showed the presence of very large crystals (Figure 1).

To understand the lack of control in selectivity, the batch of starting piperazine dihydrochloride **18** with very large crystals was suspended in ethyl acetate at 25 °C, treated with triethylamine and Boc_2O portionwise. To be noted is that a clear solution was not observed at this point because both the piperazine and $Et_3N·HCl$ are insoluble solids in ethyl acetate. Thus, the acid exchange should occur only on the surface of the crystals, driving a partial conversion to the monoprotected compound **19**. Due to its higher solubility, the compound **19** converted into the double-protected compound **21** by reaction with the Boc_2O still present. Several alternatives were tested trying to improve the process: increasing the amount of ethyl acetate to solubilise the piperazine **18**; changing the solvent and increasing the temperature. More than 100 volumes of ethyl acetate were required to get complete solubilisation. Since the undesirable dichloromethane was the only solvent better than ethyl acetate in solubilising piperazine **18**, it was decided to operate on the temperature. On stirring **18** in the presence of triethylamine for 2 h at 40 °C, cooling back to 20 °C and adding Boc_2O, the expected ratio *ca.* 95:5 mono versus diprotected was obtained. The stirring period at 40 °C seemed to be fundamental for breaking down the bigger crystals achieving a better dissolution rate, increasing the availability of the substrate and improving the acid exchange between **18** and the triethylamine. So, without the need of an extra particle size reduction step, the double protection was limited.

3.3. Screening of Coupling Agents. Using **19** as the starting material for the downstream chemistry, we investigated possible coupling agents (Scheme 5). In particular carbonyl-di-imidazole,[8] bis(*p*-nitrophenyl) carbonate,[9] triphosgene,[10] and phosgene[11] were tested.

On reacting **19** with carbonyl-di-imidazole the corresponding acylimidazole was obtained in quantitative yields, but this did not react directly with **16** if the imidazole moiety was not preliminary quaternised with iodomethane. The reaction proved to be extremely difficult to interpret by HPLC and afforded **20** in only 35% a/a. A similar behaviour was observed with bis(*p*-nitrophenyl) carbonate; the intermediate carbonate was obtained with an almost quantitative yield, but the subsequent reaction

(5) Shields, J. E.; Carpenter, F. H. *J. Am. Chem. Soc.* **1961**, *83*, 3066–3070.
(6) Atwell, G. J.; Denny, W. A. *Synthesis* **1984**, *12*, 1032–1033.
(7) Houghten, R. A.; Beckman, A.; Ostresh, J. M. *Int. J. Pept. Protein Res.* **1986**, *27* (6), 653–658.
(8) Lam, P. Y. S.; Ru, Y.; Jadhav, P. K.; Aldrich, P. E.; DeLucca, G. V.; Eyermann, C. J.; Chang, C.-H.; Emmett, G.; Holler, E. R.; et al. *J. Med. Chem.* **1996**, *39* (18), 3514–3525.
(9) Izdebski, J.; Pawlak, D. *Synthesis* **1989**, *6*, 423–425.
(10) Jacobsen, E. J.; Stelzer, L. S.; Belonga, K. L.; Carter, D. B.; Im, W. B.; Sethy, V. H.; Tang, A. H.; VonVoigtlander, P. F.; Petke, J. D. *J. Med. Chem.* **1996**, *39* (19), 3820–3836.
(11) Zeidan, T. A.; Wang, Q.; Fiebig, T.; Lewis, F. D. *J. Am. Chem. Soc.* **2007**, *129* (32), 9848–9849.

Scheme 5. **Coupling**

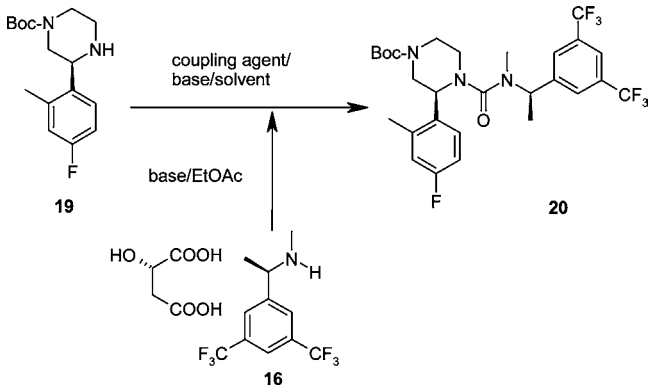

with **16** proceeded with a negligible conversion. The first trial with triphosgene gave an uncorrected yield of 78% molar versus a 49% achieved with a solution of phosgene in toluene. Even after screening a combination of solvents (acetonitrile, dichloromethane, toluene, and ethyl acetate) and bases (Et_3N, $^iPr_2NEt$), the best result was as high as an uncorrected yield of 58%. Those promising results with triphosgene convinced us to drop the less safe phosgene coupling agent.

3.4. Triphosgene Coupling Optimisation. Once triphosgene was selected as the coupling agent, all the subsequent experiments aimed to maximise both yield and purity of the final product.

The starting conditions of the process were: triphosgene (0.45 equiv) was dissolved in ethyl acetate (12 vol), and the solution was cooled to 0 °C. A solution of N-Boc protected piperazine **19** (1 equiv) and triethylamine (1.5 equiv) were added followed by a stirring period of 30 min at 0 °C. The resulting suspension was heated to reflux and treated with a solution of benzylamine **16** (1.5 equiv as free base) and triethylamine (1.2 equiv) in ethyl acetate (15 vol). The reaction mixture was kept at reflux for 6 h before being cooled to 25 °C. Among the several observed impurities, bis-benzylamine derivative **27** resulted in being the predominant one.

With the aim of reducing the total volumes of solvent, reducing the number of equivalents of triphosgene, reducing the amount of the expensive benzylamine **16**, and producing a lower formation of the main byproduct **27** (coming again from the benzylamine **16**) we carried out a design of experiment (DoE): 30 experiments; central composite design; factors: equivalents of triphosgene from 0.35 to 0.45, volumes of the solution of protected piperazine **19** from 2 to 10, equivalents of benzylamine **16** from 1.2 to 1.5, and volumes of the solution of benzylamine **16** from 5 to 15. In the end we expected to achieve also a better yield.

By interpreting the results of the DoE study we were able to understand the impact of the equivalents of triphosgene on the self-condensation of benzylamine into the bis-urea **27**, and we were able to identify the best reaction conditions to improve both yield and quality (0.38 equiv of triphosgene, 1.4 equiv of benzylamine **16**, amount of solvent not a critical factor (Figure 2)). Having identified the best conditions to minimize the impurity **27**, we further investigated the fate of the other impurities (Scheme 6). For example, the incomplete Boc protection of piperazine **18**, as made explicit in section 3.2, led to the compound **25**, due to the reaction of both piperazine nitrogens with triphosgene followed by the coupling with two benzylamine molecules. Starting piperazine **18** was found in the final isolated product as a result of deprotection of the di-Boc piperazine **21** still present at the end of the coupling. Large amounts of benzylamine gave higher conversion to the desired urea, but the excess of the reagent led to the formation of two other impurities, **25** and **26**. The triethylamine adduct **26** was also observed with a long reaction time at high temperature. Interestingly enough, in the same conditions we also identified an impurity, **28**, possibly generated by the reaction of benzylamine with triphosgene followed by the reaction with Et_3N and subsequent loss of ethylene, the same as for the formation of **26**. A low amount of triphosgene, potentially due either to incomplete addition of reagent or a too-high level of quenching water, led to another bis-urea **24**, *via* the coupling of the carbamoyl chloride **22** with the mono-Boc piperazine **19**. Following deprotection, **24** led to **29**. A short reaction time meant incomplete conversion of the carbamoyl chloride **22** that reacted with the desired urea **1**, giving a further undesired bis-urea **23** (Scheme 6).

Having understood the nature and the root cause of the impurities, we devised the reaction conditions to minimize them all. The bis-benzylamine derivative **27** was already kept under

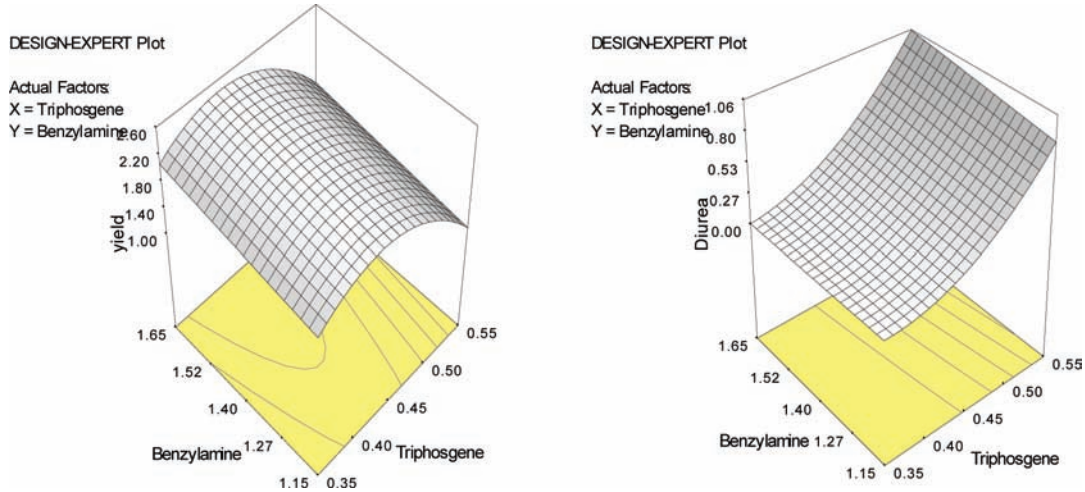

Figure 2. **Effect of equivalents of benzylamine 16 and triphosgene on conversion to desired product 20 and main impurity 27.**

Scheme 6. **Process and impurities in the triphosgene process**

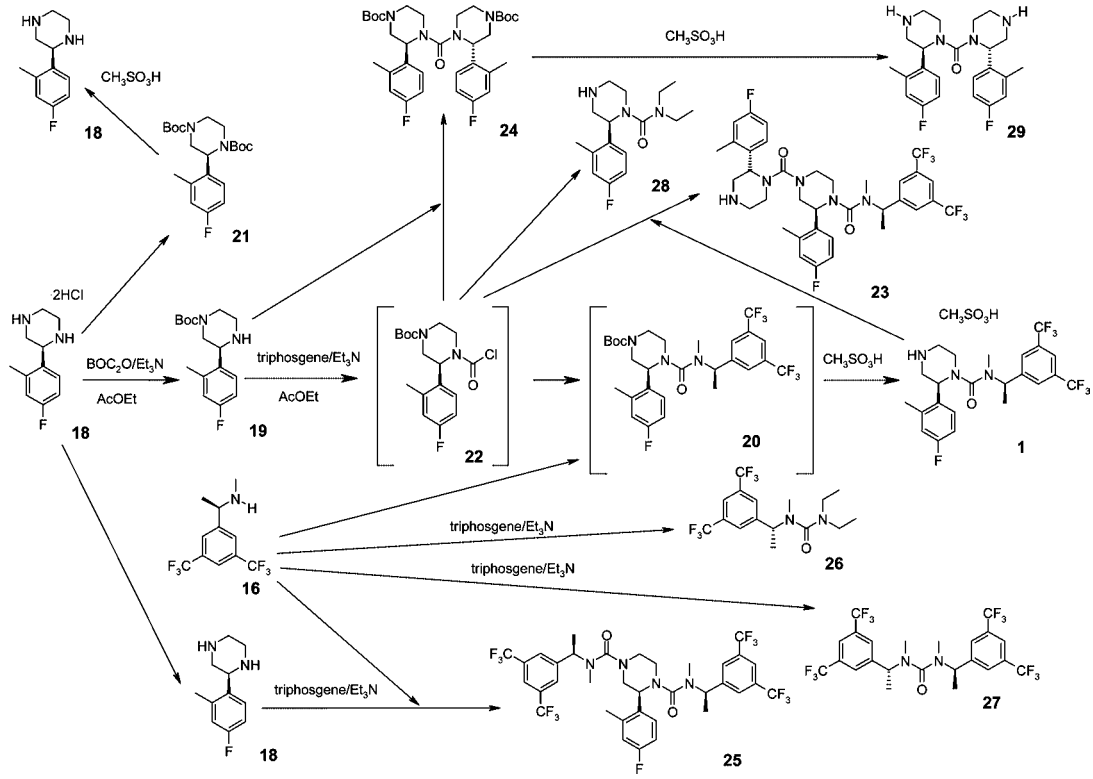

Scheme 7. **New potential alternative to triphosgene**

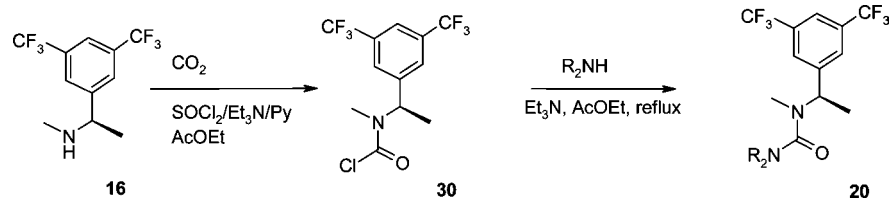

control by applying the conditions suggested by the DoE study. In addition, similarly to **27**, not having basic nitrogens, **25** and **26** also could not precipitate during the crystallisation step.

By ensuring the completeness of the formation of the carbamoyl chloride we prevented the formation of both **24** and its derivative **29**. On the other hand, the complete consumption of the carbamoyl chloride buffered the formation of **23**. The impurity **28** resulted in being only a minor one, controlled *via* the crystallisation conditions.

3.5. Deprotection. Trifluoroacetic acid in *tert*-butylmethyl ether was initially used to remove the Boc protection. However *tert*-butylmethyl ether is a potential human carcinogen,[12] and it was nicely replaced with ethyl acetate, a solvent already in use in the previous steps.

The GW597599 initial selected salt was the acetate, but it proved to be chemically unstable at temperatures above 60 °C; thus, after a salt selection screening, the mesylate was chosen as the preferred version due to an improved stability and better physical properties profile such as a higher melting point, a higher crystallinity, and a single isolated polymorph. A further advantage was the capability of methanesulphonic acid to remove the Boc group while forming the desired salt. However, a direct salt formation from the reaction gave only a moderate 26% yield, probably due to the too large excess of acid required for the deprotection, leading to a biphasing system. A higher yield of 70−75% was obtained when the intermediate salt was first washed with base and then the resulting solution treated with a stoichiometric amount of methanesulphonic acid.

3.6. Development of an Alternative to Triphosgene. As the production scale increased, the safety issues concerning the use of triphosgene[13] prompted us to reinvestigate alternative reagents, even if the preliminary work on other coupling agents was not too promising. However, we investigated the little known use of the carbon dioxide/thionyl chloride mixture[14] for the synthesis of the carbamoyl chloride. Between the two partners of the coupling reaction, piperazine **19** and the benzylamine **16**, the latter gave a higher conversion for the transformation described in Scheme 7.

The possible mechanism (Scheme 8) described in the literature[14] for the carbamoyl formation passes through an unstable intermediate triethyl ammonium salt (**31**, Scheme 8),

(12) *Toxicology and Industrial Health*; CRC Press: Boca Raton, FL, 1995; Vol. 2, No. 2, pp 119−149.
(13) Urben, P., Ed. *Bretherick's Handbook of Reactive Chemical Hazards*, 7th ed.; Academic Press: Burlington, MA, 2008; Vol. 1, pp 429−430.
(14) McGhee, W. D.; Pan, Y.; Talley, J. J. *Tetrahedron Lett.* **1994**, *35*, 839.

Scheme 8. **Initial carbamoyl chloride alternative process**

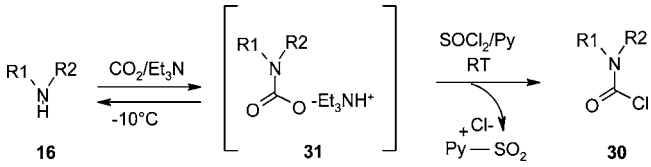

whereas the role of pyridine remained unclear, probably acting as a trap for the sulphur dioxide formed during the reaction.

It should be said that the reaction suffered from variability of yield without a clear rationale, maybe due to the instability of the salt **31** involved in the equilibrium. The reaction was improved by trapping the intermediate salt **31** in order to push the equilibrium towards completion. The use of trimethylsilyl chloride[15] was found to be the right choice, leading to a higher conversion of the starting material and a less variable profile. The resulting hypothetical trimethylsilyl species **32** forced the equilibrium between salt **31** and starting material **16** (Scheme 9), even when running the reaction at room temperature.

This three-phase reaction required intense studies to become scalable; studies focused not only on the optimization of the equivalents of reagents but also on engineering issues.

Even on small scale the rate of carbon dioxide flow appeared to be essential and required specific investigations. Reactions were performed in a closed system, namely a hydrogenation apparatus (Endeavour[16]), to check the amount of gas consumed during the reaction and to evaluate the effect of an overpressure. Additional tests using an infrared probe (Figure 3) aimed to assess the amount of carbon dioxide absorbed in the solvent. All these experiments highlighted the fact that the absorption of carbon dioxide during the equilibrium between the free secondary amine **16** and the carbamoyl acid derivative **31** (Scheme 9) was low, leading to a **16**:**30** ratio of only 19:1. A relevant absorption of carbon dioxide occurred after the addition of trimethylsilyl chloride which drove the equilibrium to the carbamoyl silane intermediate (**32**). It was also demonstrated that the carbon dioxide flow was needed all along the reaction, even after the addition of the thionyl chloride, due to its capability to remove other gases from the headspace. In fact GC−MS spectra observed very low levels of sulphur dioxide and trace quantities of hydrogen chloride in the reactor headspace, supporting the hypothesis that the carbon dioxide flow is necessary to remove sulphur dioxide, driving the equilibrium toward completion. An additional proof is shown in Figure 3; when the reaction was performed under overpressure of carbon dioxide in the closed system (Endeavour), it was faster even before the addition of TMSCl, possibly due to the higher solubility of carbon dioxide in the solvent, but slower in the second part due to the impossibility of the carbon dioxide acting as scrubber for the sulphur dioxide (Figure 3, red line). Vice versa the carbon dioxide flow (Figure 3, green line) provided a slow reaction before the addition of TMSCl, but it turned out to be much faster upon addition of TMSCl.

(15) Knausz, D.; Kolos, Z.; Meszticzky, A.; Csakvari, B. *Kemiai Kozlemenyek* **1992**, *74* (1−2), 147–159.

(16) Endeavor, Argonaut, is a system made of eight reactor vessels with independent temperature and pressure controls. It works on a maximum scale of ∼5 mL, and it permits feeding a reactant in the closed vials, monitoring the pressure trend versus time.

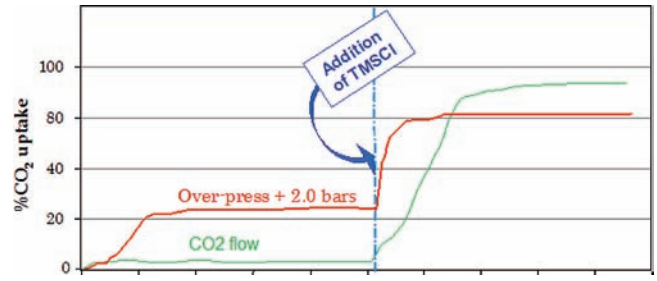

Figure 3. **Carbon dioxide uptake versus inlet pressure.**

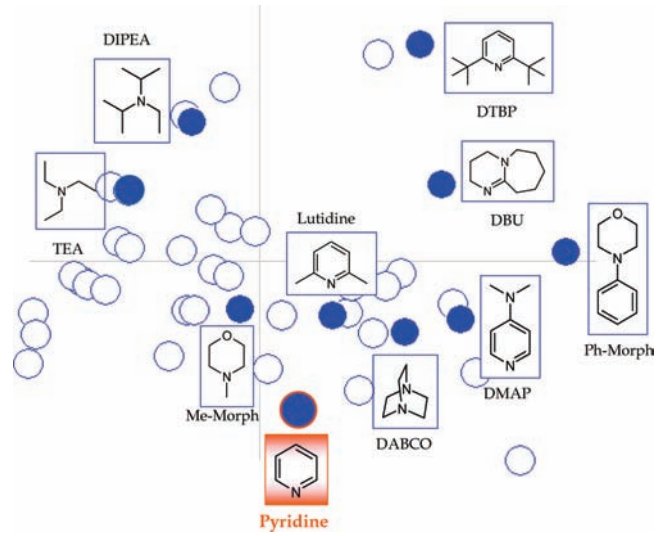

Figure 4. **Nine bases to screen were selected using a PCA viewer.**

While keeping the supply of carbon dioxide constant, a first-reagents screening was performed to simplify the procedure, with the aim of replacing pyridine with a safer base. A principal component analysis (PCA)[17] was employed to ensure diversity in reagents for the screening (Figure 4). The investigation showed that each of the two bases (triethylamine and pyridine) played a different role and that pyridine was indeed the most suitable base for the second part of the reaction.

Further DoE investigations elucidated the impact of the thionyl chloride concentration and the temperature on the overall yield. The DoE study (D-optimal design, 20 experiments, seven factors: from 1 to 2 equivalents of thionyl chloride, temperature T_1 from 0 to 25 °C before TMSCl addition, temperature T_2 from 0 to 25 °C after TMSCl addition, from 5 to 10 volumes of ethyl acetate, from 1.5 to 2.5 equivalents of triethylamine, from 1 to 2 equivalents of TMSCl, from 1.5 to 2.5 equivalents of pyridine) proved to be quite complex, due to several constraints required to ensure that regular chemistry took place: such as constant carbon dioxide flow, the total quantity of bases greater than the quantity of chloride reagents (triethylamine + pyridine > TMSCl + $SOCl_2$), and the two different temperatures to be

(17) Each class of compounds (for example solvents and reagents) can be described by relevant chemical descriptors (e.g., dielectric constant, boiling point, logP, etc.) that generate vectors in a multidimensional space. The PCA is a statistical approach that allows reducing the descriptors to three principal components; in this way, solvents that are expected to behave similarly are close in space. For a more statistical discussion: Eriksson, L., Johansson, E., Kettaneh-Wold, N., Wold, S. *Multi- and Megavariate Data Analysis, Principles and Applications*; Umetrics Academy: Umeå, Sweden, 2001; pp 43−48.

Scheme 9. **Final alternative triphosgene process**

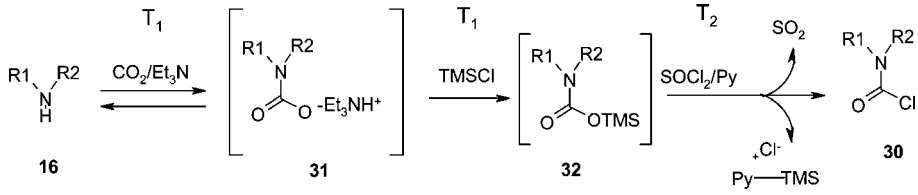

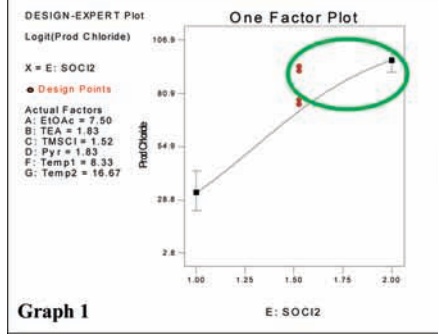

Graph 1

Influence of thionyl chloride (E)

The impact of quantity of thionyl chloride (E) is not relevant in any interaction. The plot (Graph 1) shows that the yield is higher with higher quantity. But the use of a large amount of thionyl chloride led to a very dark reaction mixture with difficulties in the work-up.

➔ The equivalents of thionyl chloride were increased from 1.3 to 1.5.

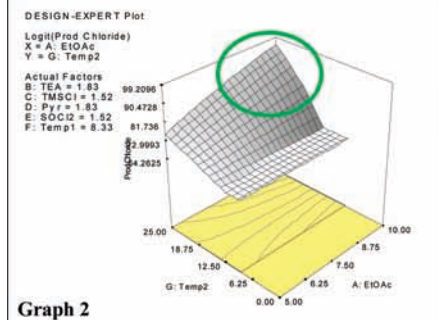

Graph 2

Interaction Volumes x T_2 (AG)

Graph 2 illustrates the relevant impact of temperature after trimethylsilyl chloride addition (T_2). The yield could drop if T_2 is decreased below 25°C.
Both volumes of ethyl acetate and T_2 should be high to maximize the yield.

➔ T_2 was maintained and carefully controlled at the 25°C while the volumes of ethyl acetate were increased to 10.

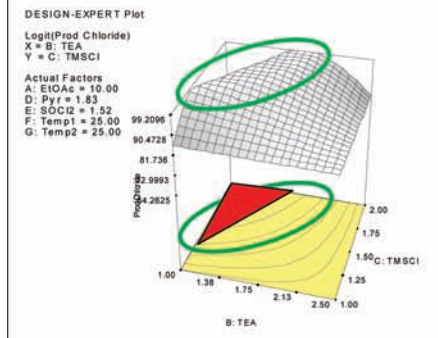

Graph 3

Interaction triethylamine x trimethylsilyl chloride (BC)

Graph 3 shows that there is a plateau area where triethylamine is low (1.0-1.5 equiv) and trimethylsilyl chloride is high (1.5-2.0 equiv), respecting the constraint (out of red area).

➔ The equivalents of trimethylsilyl chloride were increased from 1.3 to 1.5 while the equivalents of triethylamine should be decreased to below 1.5.

Note: the red area represents conditions out of constraints that were not tested for safety reasons: the equivalents of triethylamine must be higher than the equivalents of trimethylsilyl chloride to trap all the evolved HCl.

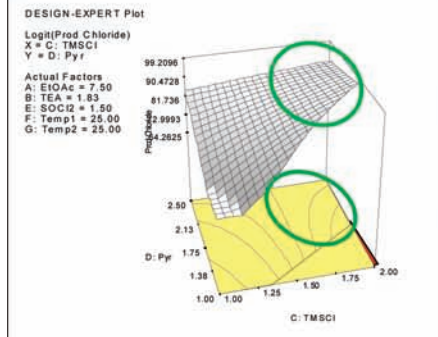

Graph 4

Interaction trimethylsilyl chloride x pyridine (CD)

The 3D-surface of Graph 4 illustrates that the yield could drop significantly if trimethylsilyl is decreased and if the amount pyridine is low.
Thus the trimethylsilyl chloride should be high (1.5-2.0 equiv) as well as the pyridine (2.0-2.5 equiv)

➔ The equivalents of trimethylsilyl chloride were increased from 1.3 to 1.5 and the amount of pyridine was maintained higher than 2.0 equiv.

Note: see Graph 3's note.

Figure 5. **Results from robustness assessment for the formation of the carbamoyl chloride (all equivalents are referred to benzylamine starting material).**

Scheme 10. **Stage 3, final manufacturing process**

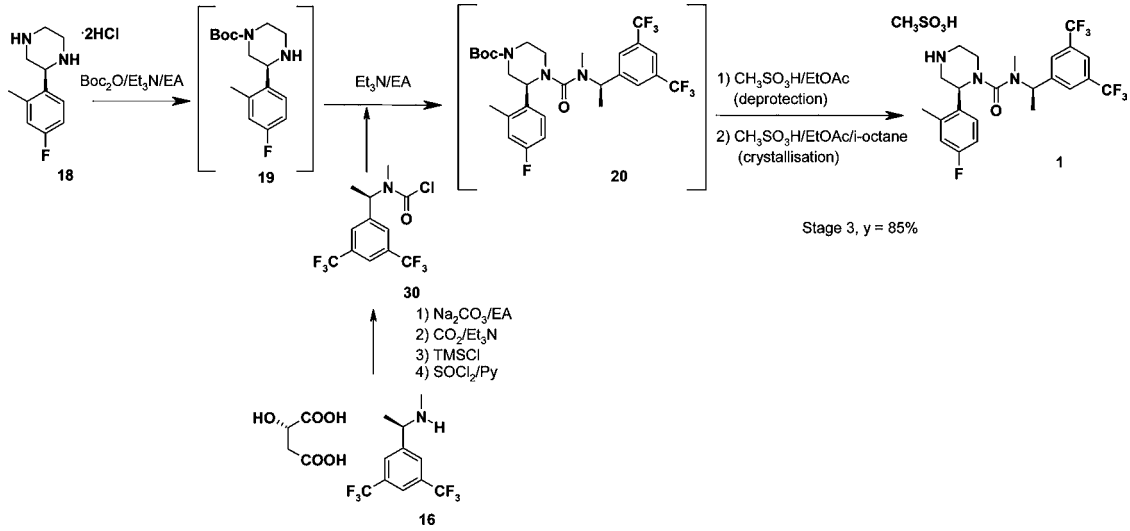

applied before and after the trimethylsilyl chloride addition ($T_1 < T_2$, Scheme 9 and Figure 5). The overall setup of experiments was very challenging, taking into account a three-phase, multistep reaction, a carbon dioxide flow rate to be kept constant, the evaporation of the solvent, the formation of volatile salts (triethylamine hydrochloride), the high exothermicity of reagents addition, the corrosion problems due to traces of hydrochloric acid gas evolution. In the end, it was possible to extract some key information from the study (Figure 5). In particular, the use of a large excess of thionyl chloride led to a faster reaction (graph 1, Figure 5). It is important to note that the amount of this reagent was not pushed to the suggested limit, because a high excess was leading to a very dark reaction mixture and to further problems in the workup procedure. Two other parameters were found important and interacting, such as the temperature after the trimethylsilyl chloride addition and the amount of solvent (graph 2, Figure 5). Those two parameters can be strongly related to the concentration of carbon dioxide in the reaction media. The temperature was maintained and carefully controlled at 25 °C, while volumes of solvent were increased up to 10. The temperature before the trimethylsilyl chloride addition was found to be less important, so that the global procedure was simplified by using a single temperature all the way through. The interactions between trimethylsilyl chloride and the two bases, triethylamine and pyridine, were also relevant (graphs 3 and 4, Figure 5).

The main points coming out of the DoE robustness assessment are summarized in Figure 5.

In summary, based on the DoE analysis, the key critical steps in this process are the initial saturation with carbon dioxide and the reaction with trimethylsilyl chloride. It is of fundamental importance to ensure the reaction is complete before the addition of thionyl chloride.

Having in hand the best reaction conditions for the carbamoyl chloride synthesis[18] of the benzylamine **16**, we managed to avoid the formation of the impurities **23**, **24**, **28**, and **29**, all based on the piperazine fragment as *per* Scheme 6. Of course, we still had to deal with the main impurities, compounds **26** and **27**, produced respectively by the reaction of the benzylamine carbamoyl chloride with the unreacted benzylamine **16** or with triethylamine. Both of them were controlled *via* the crystallisation conditions as mentioned before.

Finally, the identification of the best monoprotection conditions as described in section 3.2 minimised the presence of the impurities **18**, **21**, and **25**.

4. Conclusions

In this contribution we describe the extensive process definition made in the Chemical Development department to identify a safe,[19] robust, and scalable process for the third and last stage of the synthesis of GW597599, **1** (Scheme 10).

In the first large-scale manufacturing campaign of the three-stage process[3,4] (Scheme 11), the overall yield was 49% molar; employed were two solvents, five reactors, and a silica treatment to remove some impurities; for each kilogram of output about 190 kg of waste was generated. The final large-scale manufacturing campaign, after all the improvements described in the current paper and in the previous two publications,[3,4] took advantage of the convergent route and the new coupling reaction; on 100 kg of input, using two solvents and only three reactors and no silica treatment, a total of 58 kg of waste for each kilogram of output was produced (Figure 6 and Table 2). The yield moved up to about 80−85% molar, resulting in a final drug substance with an excellent purity greater than 98% w/w.

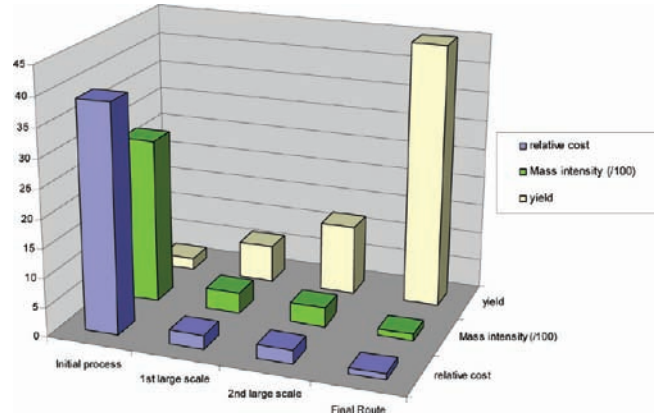

Figure 6. **Metrics of the evolution of the process.**

Scheme 11. **Overall final manufacturing process**

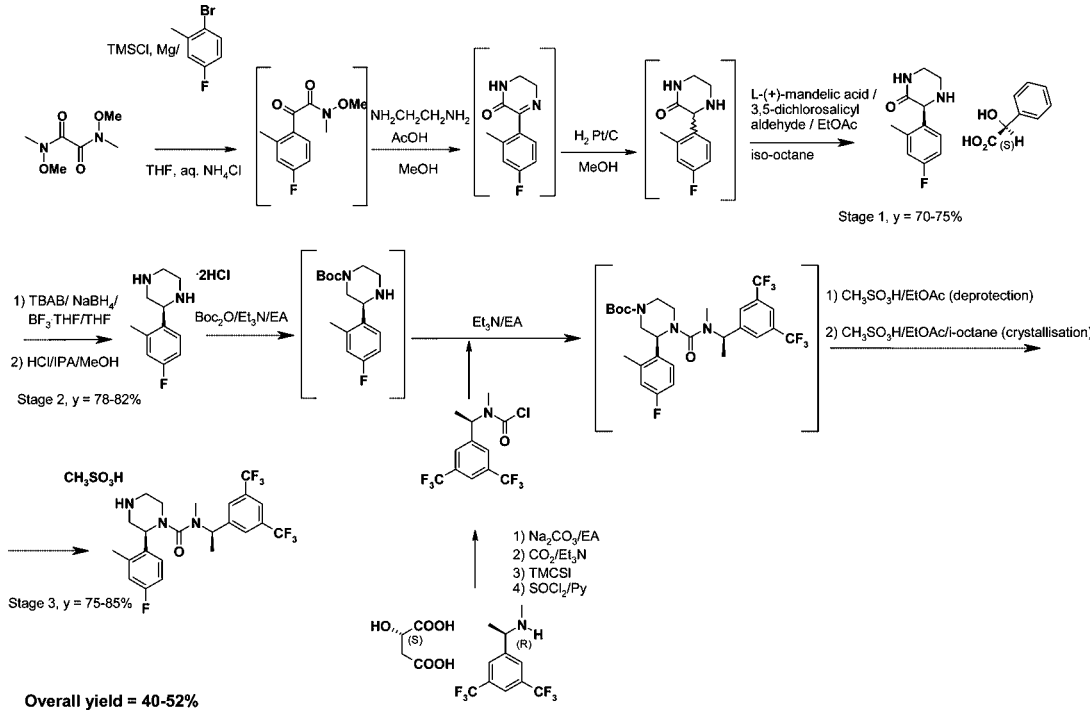

Table 2. **Metrics of the evolution of the process**

	initial process to support early toxicological studies	1st large-scale preparation to support early clinical development	2nd large-scale preparation to support late clinical development	final route to support possible launch
overall yield % mol	2	6.4	12	45
mass intensity (kg materials/1 kg output)	2830	360	327	109
relative cost of **1** to final route	39	2.4	2.3	1

Experimental Section

Generic acidic HPLC method used: column type Luna C18; mobile phase A: 0.05% TFA/water and B: 0.05% TFA/acetonitrile; gradient: 0 min 100% A to 8 min 95% B; flow 1 mL/min; column temperature 40 °C; detector UV DAD @ 220 nm.

1,1-Dimethylethyl (3*S*)-3-(4-fluoro-2-methylphenyl)-1-piperazinecarboxylate 19. Piperazine dihydrochloride **18** (600 g, 2.2 mol) was suspended in ethyl acetate (8400 mL), then triethylamine (732 mL, 5.25 mol) was added. The mixture was stirred at 40 °C for 2 h and then cooled to 20 °C, and a solution of di-*tert*-butyl dicarbonate (Boc_2O, 480 g, 2.2 mol) in ethyl acetate (2400 mL) was added over 1.5 h, maintaining a very fast stirring rate. The suspension was stirred at 20 °C for 15 min. Water (1800 mL) was added, and the aqueous layer was separated. After two further washes with water (2 × 1800 mL), the organic phase was concentrated under vacuum to 1500 mL, diluted with ethyl acetate (3600 mL), and concentrated again to 1500 mL. The solution was finally cooled to 20 °C and used as such in the next step.

^{1}H NMR (400 MHz, DMSO-d_6) δ 1.42 (s, 9H); 2.35 (s, 3H); 2.4−2.6 (bm, 2H); 2.69 (td, J = 11.7, 2.5 Hz, 1H); 2.82 (bt, J = 12.0 Hz, 1H); 2.97 (dt, J = 11.4, 2.0 Hz, 1H); 3.71 (dd, J = 10.4, 2.4 Hz, 1); 3.86 (m, 2H); 6.97 (m, 2H); 7.54 (dd, J = 8.3, 6.3 Hz, 1H).

MS (ES$^+$) *m*/*z* 295.4 (MH$^+$); generic acidic HPLC, retention time 3.7 min; purity ∼ 95% a/a.

Bis(1,1-dimethylethyl) (2*S*)-2-(4-fluoro-2-methylphenyl)-1,4-piperazinedicarboxylate 21: ^{1}H NMR (400 MHz, DMSO-d_6) δ 1.23 (s, 9H); 1.30 (bs, 9H); 2.32 (s, 3H); 3.27 (m, 1H); 3.5−3.7 (m, 4H); 3.89 (dt, J = 13.7, 4.5 Hz, 1H); 5.03 (t, J = 5.3 Hz, 1H); 6.95 (td, J = 8.7, 2.7 Hz, 1H); 7.01 (dd, J = 10.1, 2.7 Hz, 1H); 7.19 (dd, J = 8.2, 6.2 Hz, 1H).

MS (ES$^+$) *m*/*z* 395.5 (MH$^+$); generic acidic HPLC, retention time 6.4 min; purity ∼ 90% a/a.

1,1-Dimethylethyl (3*S*)-4-{[{(1*R*)-1-[3,5-bis(trifluoromethyl)phenyl]ethyl}(methyl)amino]carbonyl}-3-(4-fluoro-2-methylphenyl)-1-piperazinecarboxylate 20 (Initial Method). Triphosgene (156 g, 0.52 mol) was dissolved in ethyl acetate (4800 mL) under nitrogen. The solution was cooled to 0 °C. A solution of **19** (equivalent to 400 g of **19**, 1.36 mol) and triethylamine (285 mL, 2 mol) was added over 30 min. The mixture was stirred at 0 °C for 30 min, then the suspension was heated to reflux, and a solution of **16** (free base, 1.9 mol) and triethylamine (226 mL, 1.62 mol) in ethyl acetate (5900 mL) was added over 15 min. The reaction mixture was stirred at reflux for 6 h then cooled

(18) Bientinesi, I.; Cimarosti, Z.; Guercio, G.; Leroi, C.; Perboni, A. Patent WO 2007048642, 2007.
(19) See Supporting Information.

to 25 °C. An aqueous solution of sodium hydroxide 10% (3200 mL) was added. The basic aqueous phase was discharged, and HCl 4% (4000 mL) was added. After discharging the acid aqueous layer, the organic mixture was washed three times with NaCl 13% w/w (2000 mL). The solution was evaporated to dryness to obtain the desired product (920 g, purity about 85%) to be used as such in the synthesis of compound **1**.

^{1}H NMR (600 MHz, $CDCl_3$) δ 1.48 (s, 9H); 1.54 (d, J = 7.1 Hz, 3H); 2.43 (s, 3H); 2.78 (s, 3H); 3.04−3.15 (m, 2H); 3.26−3.37 (m, 2H); 3.80−4.03 (m, 2H); 4.58 (bs, 1H); 5.59 (q, J = 7.2 Hz, 1H); 6.81 (t, J = 8.1 Hz, 1H); 6.88 (d, J = 9.9 Hz, 1H); 7.20 (dd, J = 8.1, 5.9 Hz, 1H); 7.54 (bs, 2H); 7.75 (bs, 1H).

MS (ES^+) *m/z* 592.6 (MH^+); generic acidic HPLC, retention time 7.4 min; purity ∼ 90% a/a.

(2*S*)-*N*-{(1*R*)-1-[3,5-Bis(trifluoromethyl)phenyl]ethyl}-2-(4-fluoro-2-methylphenyl)-4-{[(2*S*)-2-(4-fluoro-2-methylphenyl)-1-piperazinyl]carbonyl}-*N*-methyl-1-piperazinecarboxamide 23: ^{1}H NMR (600 MHz, DMSO-d_6) δ 1.51 (d, J = 7.1 Hz, 3H); 2.33 (s, 6H); 2.52 (dd, J = 12.9, 8.8 Hz, 1H); 2.59 (s, 3H); 2.67−2.76 (m, 2H); 2.76−2.87 (m, 2H); 2.94−3.03 (m, 1H); 3.06−3.12 (m, 1H); 3.29 (dd, J = 13.2, 9.6 Hz, 1H); 3.33−3.40 (m, 2H); 3.53−3.63 (m, 2H); 4.27 (dd, J = 8.8, 3.3 Hz, 1H); 4.49 (dd, J = 8.9, 3.4 Hz, 1H); 5.20 (q, J = 6.9 Hz, 1H); 6.66 (t, J = 8.1 Hz, 1H); 6.86 (td, J = 8.4, 2.6 Hz, 1H); 6.93−6.97 (m, 2H); 7.17 (dd, J = 8.8, 6.0 Hz, 1H); 7.43 (dd, J = 8.8, 6.3 Hz, 1H); 7.71 (bs, 2H); 7.96 (bs, 1H).

MS (ES^+) *m/z* 712.7 (MH^+); generic acidic HPLC, retention time 5.7 min; purity ∼ 90% a/a.

Bis(1,1-dimethylethyl) (3*S*,3′*S*)-4,4′-(oxomethanediyl)bis[3-(4-fluoro-2-methylphenyl)-1-piperazinecarboxylate] 24: ^{1}H NMR (400 MHz, DMSO-d_6 at 70 °C) δ 1.47 (2s, 18H); 2.31 (s, 3H); 3.5−3.9 (bm, 6H); 5.03 (t, 1H); 6.9−7.0 (m, 2H); 7.18 (m, 1H).

MS (ES^+) *m/z* 615.7 (MH^+); generic acidic HPLC, retention time 7.2 min; purity ∼ 90% a/a.

(2*S*)-*N*,*N*′-Bis{(1*R*)-1-[3,5-bis(trifluoromethyl)phenyl]ethyl}-2-(4-fluoro-2-methylphenyl)-*N*,*N*′-dimethyl-1,4-piperazinedicarboxamide 25: ^{1}H NMR (600 MHz, DMSO-d_6) δ 1.50 (d, J = 6.9 Hz, 3H); 1.55 (d, J = 7.1 Hz, 3H); 2.31 (s, 3H); 2.62 (s, 3H); 2.67 (s, 3H); 2.93 (dd, J = 13.2, 10.7 Hz, 1H); 3.03−3.09 (m, 1H); 3.25−3.31 (m, 1H); 3.42 (dd, J = 13.0, 3.2 Hz, 1H); 3.44−3.48 (m, 1H); 3.53−3.59 (m, 1H); 4.57 (dd, J = 10.4, 3.8 Hz, 1H); 5.18 (q, J = 7.1 Hz, 1H); 5.25 (q, J = 6.9 Hz, 1H); 6.81 (dt, J = 8.4, 2.5 Hz, 1H); 6.95 (dd, J = 10.0, 2.6 Hz, 1H); 7.27 (dd, J = 8.5, 6.0 Hz, 1H); 7.72 (bs, 2H); 7.97 (bs, 2H); 7.98 (bs, 1H); 8.00 (bs, 1H).

MS (ES^+) *m/z* 789.7 (MH^+); generic acidic HPLC, retention time 7.9 min; purity > 99% a/a.

***N*-{(1*R*)-1-[3,5-Bis(trifluoromethyl)phenyl]ethyl}-*N*′,*N*′-diethyl-*N*-methylurea 26:** ^{1}H NMR (600 MHz, DMSO-d_6) δ 1.03 (t, J = 7.1 Hz, 6H); 1.54 (d, J = 6.9 Hz, 3H); 2.54 (s, 3H); 3.11 (q, J = 7.0 Hz, 4H); 5.10 (q, J = 6.8 Hz, 1H); 7.92 (bs, 2H); 7.94 (bs, 1H).

MS (ES^+) *m/z* 371.34 (MH^+); generic acidic HPLC, retention time 6.5 min; purity ∼ 90% a/a.

***N*,*N*′-Bis{(1*R*)-1-[3,5-bis(trifluoromethyl)phenyl]ethyl}-*N*,*N*′-dimethylurea 27:** ^{1}H NMR (400 MHz, DMSO-d_6) δ 1.58 (d, J = 7.0 Hz, 6H); 2.67 (s, 6H); 5.05 (q, J = 7.0 Hz, 2H); 7.92 (bs, 4H); 7.97 (bs, 2H).

MS (ES^+) *m/z* 569.4 (MH^+); generic acidic HPLC, retention time 7.7 min; purity > 90% a/a.

(2*S*)-*N*,*N*-Diethyl-2-(4-fluoro-2-methylphenyl)-1-piperazinecarboxamide 28: ^{1}H NMR (600 MHz, HPLC−NMR, D_2O/ACN) δ 0.92 (t, J = 7.3 Hz, 6H); 2.31 (s, 3H); 2.99 (m, 2H); 3.30 (m, 5H); 6.88 (m, 2H); 7.29 (m, 1H).

MS (ES^+) *m/z* 294.38 (MH^+); HPLC Zorbax Eclipse XDB C8; mobile phase A: water and B: acetonitrile; gradient: 0 min 55% A to 18 min 20% A. Flow 1 mL/min; detector UV DAD @215 nm. Retention time 2.00 min. Purity ∼ 90% a/a.

(2*S*,2′*S*)-1,1′-(Oxomethanediyl)bis[2-(4-fluoro-2-methylphenyl)piperazine] 29: ^{1}H NMR (600 MHz, HPLC−NMR, D_2O/ACN) δ 2.20 (s, 6H); 3.08−3.13 (m, 2H); 3.22−3.27 (m, 2H); 3.31−3.37 (m, 2H); 3.38−3.44 (m, 2H); 3.64−3.70 (m, 2H); 3.80−3.86 (m, 2H); 4.73 (dd, J = 11.2, 3.5 Hz, 2H); 6.83−6.88 (m, 2H); 6.90 (d, J = 9.9 Hz, 2H); 7.06−7.14 (m, 2H).

MS (ES^+) *m/z* 415.5 (MH^+); generic acidic HPLC, retention time 2.9 min; purity > 90% a/a.

{(1*R*)-1-[3,5-Bis(trifluoromethyl)phenyl]ethyl}methylcarbamic Chloride 30. Benzylamine malate **16** (1140 g, 2.81 mol) was suspended at 20 °C in ethyl acetate (3400 mL). Na_2CO_3 15% (3400 mL) was added, and the mixture was stirred until dissolution. The phases were separated, and the organic layer was washed with NaCl 20% w/w (3400 mL). The solution was concentrated to 2100 mL, ethyl acetate (3000 mL) was added, and the solution was concentrated again to 2100 mL. Further ethyl acetate (3000 mL) was added. A cycle of vacuum and CO_2 was applied to the vessel, then a CO_2 flow was maintained for the whole process. Et_3N (516 mL, 3.7 mol) was added, and the reaction mixture was stirred at 20 °C for 30 min. Trimethylsilyl chloride (540 mL, 4.25 mol) was added over 30 min (exothermic step), and the reaction mixture was stirred for a further 30 min at 20 °C. Pyridine (462 mL, 5.7 mol) was added followed by a 20 min addition of thionyl chloride (306 mL, 4.2 mol). The reaction mixture was stirred at 20 °C for 6 h under a CO_2 atmosphere. The reaction mixture was washed twice with 28% aqueous racemic malic acid (2 × 680 mL). The organic layer was washed with water (3000 mL) and then with Na_2CO_3 15% w/w (3000 mL). Ethyl acetate (3600 mL) was added, and the solution was concentrated to 1800 mL and used as such in the next step.

^{1}H NMR (600 MHz, $CDCl_3$) δ 1.67−1.74 (m, 3H), 2.89 (bs, 3H), 5.73−5.83 (m, 1H), 7.75 (bs, 2H), 7.87 (bs, 1H).

MS (ES^+) *m/z* 334.66 (MH^+); HPLC column type X-Terra RP18; mobile phase A ammonium hydrogen carbonate 5 mM pH = 10/acetonitrile 90/10% v/v and B ammonium hydrogen carbonate 5 mM pH = 10/acetonitrile 10/90% v/v; gradient: 0 min 58% B to 6 min 63% B then to 7 min 100% B. flow 1 mL/min; column temperature 40 °C; detector UV DAD @210 nm. Retention time 6.2 min. Purity > 90% a/a.

1,1-Dimethylethyl (3*S*)-4-{[{(1*R*)-1-[3,5-bis(trifluoromethyl)phenyl]ethyl}(methyl)amino]carbonyl}-3-(4-fluoro-2-methylphenyl)-1-piperazinecarboxylate 20 (Final Method). A solution of **30** was added at 25 °C to a mixture of solution **19**

and Et_3N (408 mL, 2.93 mol). The mixture was heated at reflux for at least 19 h then cooled to 25 °C. Diethylamine (66 mL, 0.64 mol) was added, and the solution was stirred for 1 h to quench the unreacted **30**. Aqueous NaCl 20% w/w (1200 mL) was added, the phases were separated, and the solution was used as such in the next step.

^{1}H NMR (600 MHz, $CDCl_3$) δ 1.48 (s, 9H), 1.54 (d, J = 7.1 Hz, 3H), 2.43 (s, 3H), 2.78 (s, 3H), 3.04−3.15 (m, 2H), 3.26−3.37 (m, 2H), 3.80−4.03 (m, 2H), 4.58 (bs, 1H), 5.59 (q, J = 7.2 Hz, 1H), 6.81 (t, J = 8.1 Hz, 1H), 6.88 (d, J = 9.9 Hz, 1H), 7.20 (dd, J = 8.1, 5.9 Hz, 1H), 7.54 (bs, 2H), 7.75 (bs, 1H).

MS (ES^+) m/z 592.6 (MH^+); generic acidic HPLC, retention time 7.4 min; purity ∼ 90% a/a.

(2*S*)-*N*-{(1*R*)-1-[3,5-Bis(trifluoromethyl)phenyl]ethyl}-2-(4-fluoro-2-methylphenyl)-*N*-methyl-1-piperazinecarboxamide Methanesulphonate 1. To the organic phase of **20**, $MeSO_3H$ (720 mL, 11.1 mol) was added over 10 min, and the mixture was heated at 40 °C and stirred for 1 h. Ethyl acetate (3000 mL) was added followed by NH_3 (13%, 2400 mL). The phases were separated, and the organic layer was washed with water (2 × 2400 mL). The reaction mixture was concentrated to 1800 mL, ethyl acetate (6000 mL) was added, and the mixture was concentrated finally to 3600 mL. Methanesulphonic acid (144 mL, 2.2 mol) was added dropwise at 25 °C and the solution seeded with **1** (3 g). Isooctane (7200 mL) was added over 90 min. The suspension was stirred for at least 6−8 h and filtered, and the solid was washed three times with an ethyl acetate/isooctane 1:2 mixture (3 × 1800 mL). The resulting solid was dried under vacuum at 40 °C for at least 3 h, obtaining 1100 g of **1** (98% w/w purity, theoretical yield = 85% from **18**).

^{1}H NMR (600 MHz, DMSO-d_6) δ 1.48 (d, J = 6.9 Hz, 3H); 2.31 (s, 3H); 2.39 (s, 3H); 2.74 (s, 3H); 2.95 (t, J = 12.2 Hz, 1H); 3.00−3.06 (m, 1H); 3.27 (dd, J = 12.5, 2.3 Hz, 1H); 3.28−3.35 (m, 1H); 3.38−3.43 (m, 1H); 3.47 (dt, J = 13.3, 3.1 Hz, 1H); 4.49 (dd, J = 11.8, 3.3 Hz, 1H); 5.35 (q, J = 6.5 Hz, 1H); 6.84 (td, J = 8.4, 2.6 Hz, 1H); 7.01 (dd, J = 10.2, 2.7 Hz, 1H); 7.29 (dd, J = 8.5, 6.0 Hz, 1H); 7.71 (bs, 2H); 8.02 (bs, 1H); 8.71 (bs, 1H); 9.02 (bs, 1H).

ES^+: m/z 492 $[MH - CH_3SO_3H]^+$, 341, 221; ES^-: m/z 586 $[M - H]^-$; 95 $[CH_3SO_3]^-$.

^{13}C NMR (150 MHz, DMSO-d_6) δ 16.37, 18.81, 30.54, 39.79, 42.41, 45.70, 46.58, 52.41, 53.42, 112.48, 116.55, 121.02, 123.19 (d), 127.19, 127.44 (d), 130.34 (d), 134.00, 138.56, 144.79, 160.89, 163.2.

IR (Nujol mull, cm^{-1}): 1653 (str. C═O), 1600 (str. C═C aromatic) (cm^{-1}).

HPLC column type Betabasic C18; mobile phase A: buffer ammonium hydrogen carbonate 5 mM pH = 10/methanol 40/60% v/v and B buffer ammonium hydrogen carbonate 5 mM pH = 10/methanol 10/90% v/v; gradient: 0 min 100% A to 20 min 100% B. flow 1 mL/min; column temperature 40 °C; detector UV DAD @210 nm. Retention times **1**: 13 min, purity >98%.

HPLC column type Chiralpack AD; mobile phase *n*-hexane/ethanol 86/14% v/v + 0.2% v/v purified water; flow 1 mL/min; column temperature 25 °C; detector UV DAD @210 nm. Retention time **1**: 4.56 min and opposite enantiomer 4.15 min, other diastereomers 5.20 and 14.2 min, respectively.

Acknowledgment

We thank Lucilla Turco for the spectroscopic characterisation of the compounds and for valuable discussions. We also thank Giulio Camurri and Luca Martini for the HPLC method development, Francois Ricard for computational modelling studies and Gilles Laval for his support defining the process.

Supporting Information Available

Process safety evaluation of the process and chiral HPLC of **1**. This information is available free of charge via the Internet at http://pubs.acs.org.

Received for review August 3, 2009.

OP9002032